BIOCHEMISTRY
including biophysical chemistry & molecular biology

ARTICLE

pubs.acs.org/biochemistry

Mass Spectrometry Reveals That the Antibiotic Simocyclinone D8 Binds to DNA Gyrase in a "Bent-Over" Conformation: Evidence of Positive Cooperativity in Binding

Marcus J. Edwards,[†,||] Mark A. Williams,[‡] Anthony Maxwell,[†] and Adam R. McKay*[,§]

[†]Department of Biological Chemistry, John Innes Centre, Norwich Research Park, Colney, Norwich NR4 7UH, United Kingdom

[‡]Biophysics Centre, Institute of Structural and Molecular Biology, Department of Biological Sciences, Birkbeck, University of London, Malet Street, London WC1E 7HX, United Kingdom

[§]Department of Chemistry, University College London, London WC1H 0AJ, United Kingdom

ABSTRACT: DNA topoisomerases are enzymes that control DNA topology and are vital targets for antimicrobial and anticancer drugs. Here we present a mass spectrometry study of complexes formed between the A subunit of the topoisomerase DNA gyrase and the bifunctional inhibitor simocyclinone D8 (SD8), an antibiotic isolated from *Streptomyces*. These studies show that, in an alternative mode of interaction to that found by X-ray crystallography, each subunit binds a single bifunctional inhibitor with separate binding pockets for the two ends of SD8. The gyrase subunits form constitutive dimers, and fractional occupancies of inhibitor-bound states show that there is strong allosteric cooperativity in the binding of two bifunctional ligands to the dimer. We show that the mass spectrometry data can be fitted to a general model of cooperative binding via an extension of the "tight-binding" approach, providing a rigorous determination of the dissociation constants and degree of cooperativity. This general approach will be applicable to other systems with multiple binding sites and highlights mass spectrometry's role as a powerful emerging tool for unraveling the complexities of biomolecular interactions.

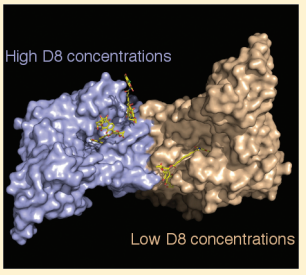

Protein−ligand interactions are of paramount importance in biology, and determination of their stoichiometries, affinities, and dynamic behavior is key to understanding biological processes. A variety of structural and biophysical methods have been applied to these systems; in particular, X-ray crystallography has proven to be of immense value. However, despite revealing atomic details of the ligand-binding sites, the structures obtained are a "snapshot" and do not necessarily provide a complete picture of possible binding modes, nor do they provide information about the strength of the interactions, aspects of which are often crucial to their function.

Mass spectrometry (MS) offers a complementary approach to high-resolution structural methods. It has been established that gas-phase noncovalent protein complexes can retain the structural features seen in solution, even after relatively long periods of time (15−30 ms),[1] and that under carefully controlled conditions the gas-phase structures of proteins and protein complexes resemble those determined in solution by nuclear magnetic resonance (NMR) or in the solid state by X-ray crystallography.[1−6] In addition, many studies have convincingly shown that important information about protein−protein, protein−oligonucleotide, and protein−ligand interactions can be determined.[7−12] For example, MS provides a rapid, straightforward evaluation of stoichiometries and a quantitative determination of binding affinities,[13−15] both of which are often time-consuming and challenging to obtain by other methods.

Here we report a MS study of the interactions between the antibiotic simocyclinone SD8 and the topoisomerase DNA gyrase. DNA topoisomerases are enzymes that catalyze changes in DNA topology in all cells,[16,17] via transient breakage of DNA in one or both strands and the formation of a covalent enzyme−DNA intermediate. All topoisomerases can relax supercoiled DNA, but only DNA gyrase, an essential enzyme in all bacteria, can introduce supercoils into relaxed DNA at the expense of ATP hydrolysis. Gyrase consists of two subunits, GyrA (97 kDa in *Escherichia coli*), which is mainly involved in DNA binding, and GyrB (90 kDa in *E. coli*), which contains the ATPase activity, with the active enzyme forming an A_2B_2 complex.[18]

Because of their essential nature and the fact that they stabilize breaks in DNA, topoisomerases have become important drug targets for both antibacterial agents and anticancer drugs.[19−21] DNA gyrase is the target of a number of antibacterials, including the fluoroquinolones, such as ciprofloxacin, and the aminocoumarins, such as novobiocin. Recently, the aminocoumarin simocyclinone D8 (SD8) (Figure 1) has been identified as a gyrase-specific antibiotic. Simocyclinones are hybrid antibiotics containing both aminocoumarin (AC) and polyketide (PK) groups at opposite ends of an elongated molecule.[22−25] Whereas novobiocin and other aminocoumarins bind to the GyrB subunit and inhibit the ATPase activity, simocyclinones bind to GyrA and prevent the binding of DNA to GyrA.[22] This novel mode of action presents new opportunities for drug development.

Received: October 20, 2010
Revised: February 16, 2011
Published: February 22, 2011

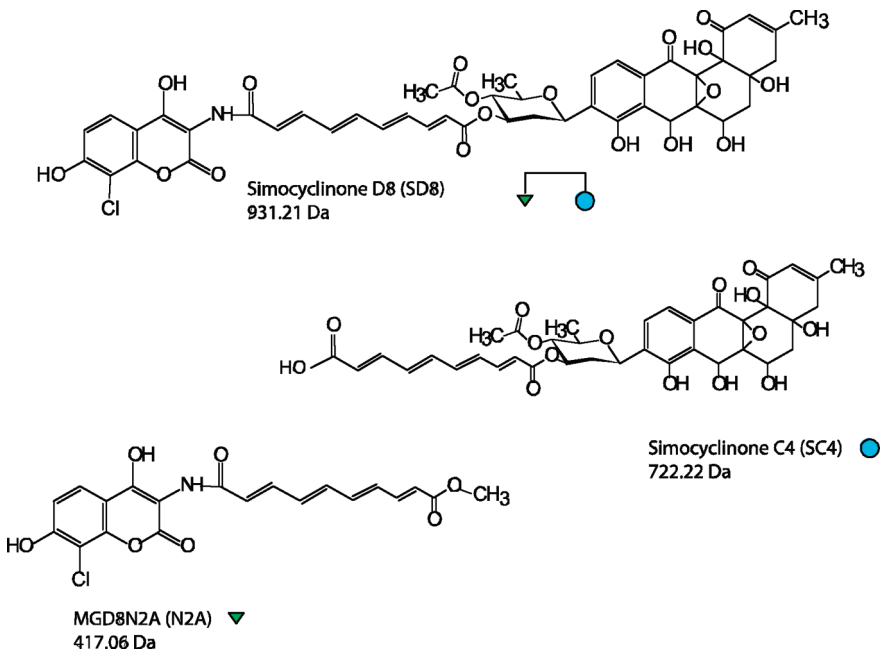

Figure 1. Chemical structures of SD8 and monofunctional fragments, each containing one of the two active binding ends of SD8, which were isolated from the biosynthetic pathway for SD8 (SC4) or chemically synthesized (N2A). In later figures, each structure will be represented by a cartoon in which a downward-pointing green triangle depicts the aminocoumarin N2A, a cyan circle the polyketide SC4, and a downward-pointing green triangle linked to a cyan circle the bifunctional SD8.

We have recently reported the crystal structure of the complex between SD8 and the N-terminal domain of GyrA (GyrA59).[26] This revealed that each GyrA monomer can bind the aminocoumarin (AC) and polyketide (PK) ends of SD8 in separate binding pockets, which are distinct from the binding pocket for quinolones. The crystal structure demonstrated that SD8 at high concentration induces tetramerization of GyrA by forming a bridge between two homodimers. This tetramer was confirmed by analytical ultracentrifugation and mass spectrometry to be not just a crystallization artifact but also present in solution under similar conditions.[26]

This study, while confirming the crystallographic 1:1 stoichiometry, shows that the major solution state species at lower, pharmaceutically relevant, ligand concentrations are GyrA59 dimers bound to one or two SD8 ligands. MS experiments with fragments of the antibiotic (Figure 1) have established that both the AC and PK ends of the inhibitor are required for tight binding. In addition, our titration experiments have established that SD8 exhibits a previously undetermined positive allosteric cooperativity in binding to GyrA59. Cooperative effects play a central role in many aspects of biology and are increasingly important in drug discovery.[27,28] However, elucidating the subtle complexity of such interactions represents a considerable challenge. The ability of mass spectrometry to quantitate the populations of each species in a reaction mixture has been most widely applied to the study of metal−peptide interactions.[29] However, the growing application of MS to larger biological systems makes it a powerful emerging tool for unraveling the complexities of cooperative interactions.[30,31] Here we demonstrate that mass spectrometry data can be directly fitted to the equations describing the population of each species in a general model of cooperative binding,[27] providing a rigorous determination of the dissociation constants and degree of cooperativity in the binding of SD8 to GyrA59. Such behavior explains the reduced inhibitory activity observed in *in vitro* assays using SD8 fragments and unambiguously demonstrates that both ends of the SD8 drug interact simultaneously with GyrA. Taken together, the MS data support a model in which SD8 binds in an alternative "bent-over" conformation, previously thought to exist, with the AC and PK ends binding to the same GyrA monomer.[26]

EXPERIMENTAL PROCEDURES

Proteins, DNA, and Drugs. Full-length GyrA from *E. coli* was purified using a protocol similar to that described previously,[32] omitting the ammonium sulfate precipitation step. GyrA59 was purified using a protocol similar to that described previously,[33] omitting the ammonium sulfate precipitation step and including a phenyl-Sepharose column between the heparin Sepharose and MonoQ columns.[34] Relaxed pBR322 DNA was purchased from Inspiralis Ltd. Simocyclinone D8 (SD8), simocyclinone SC4, and MGD8N2A were obtained from H.-P. Fiedler and A. Zeeck. All three compounds were dissolved in dimethyl sulfoxide (DMSO).

Mass Spectrometry. Proteins (44 μM monomer concentration) were buffer-exchanged into 250 mM ammonium acetate (pH 7.5) using mini gel filtration columns (Bio-Rad, Hercules, CA). SD8 stock solutions were prepared in DMSO; the final protein/antibiotic solutions contained not more than 1.6% DMSO. Ions were generated by nanoflow electrospray ionization and spectra recorded on an LCT Premier XE mass spectrometer (Waters, Manchester, U.K.) modified for high-mass operation. Nitrogen gas was leaked into the initial stages of the vacuum chamber to aid in the radial focusing of high-mass ions. Typically, nanospray ionization was performed using 2−3 μL of an aqueous protein solution and a capillary voltage of 1.6−1.9 kV.

Spectra were calibrated externally using an aqueous 33 mg/mL solution of cesium chloride.

Tight-Binding Analysis for Multiple Bound Dimer Species. For single-site binding, the standard approach to analysis of inhibition in the "tight-binding" limit, i.e., in which a significant fraction of the total ligand is bound to the target protein, involves nonlinear regression to the quadratic equation that describes the fraction of binding sites occupied (or reduction in velocity of a reaction) in terms total ligand (S_{tot}) and total protein concentrations.[35,36] We have used an analogous approach to determine the binding constants in this case. The mass spectrometry data provide information about the fractional populations of protein dimers in the apo state (T_0), bound to one ligand (T_1), and bound to two ligands (T_2) for any experimental combination of S_{tot} and dimer concentration D_{tot}.

It is straightforward to write down the expressions for the fractional occupancies [using the definitions of equilibrium constants K_1 and K_2 of the first and second binding events, respectively (eqs 7 and 8), and cooperativity α (eq 9)] in terms of the free ligand concentration (S):

$$T_0 = 1/(1 + 2K_1S + \alpha K_1^2S^2) \quad (1)$$

$$T_1 = (2K_1S)/(1 + 2K_1S + \alpha K_1^2S^2) \quad (2)$$

$$T_2 = (\alpha K_1^2S^2)/(1 + 2K_1S + \alpha K_1^2S^2) \quad (3)$$

Some previous attempts to utilize MS data to analyze cooperativity have used the fact that the concentration of free ligand, S, can be estimated from the experimental data using eq 10, plotted the experimental data for T_0, T_1, and T_2 versus S, and simulated curves using a variety of values for equilibrium constants to find a match to the experimental data. While this approach can, in principle, be formalized into an iterative fitting procedure, it is known from studies of single-site binding that in the tight-binding limit, using such indirect estimates for S results in both systematic and larger statistical errors in the fitted parameters.[37] Essentially, the difficulty is that in the case of high-affinity binding, S is always small and, because its indirect estimate is significantly affected by combined errors in the measurement of T_1 and T_2, often has an unphysical negative value. A further approach in the literature is to estimate α alone from the relationship $\alpha = (4T_0T_2)/T_1^2$ at a single concentration.[31] This is effective if both α and the affinities, which are not available from this analysis, are not too large. However, with that approach in cases of high affinity, or highly cooperative binding or high concentrations of ligand, T_1 is depleted and the error in its measurement very strongly affects the reliability of estimates of the degree of cooperativity.

For a tight-binding approach, we rewrite eqs 1−3 in terms of the experimentally measured total ligand concentration (S_{tot}), by substituting the expression for S from eq 10 into eqs 1−3 and rearranging. We obtain three cubic equations, each of which describes the population of one species in terms of S_{tot}, D_{tot}, and the equilibrium constant K_1 and cooperativity α:

$$4K_1^2D_{tot}^2(1-\alpha)T_0^3 + 4K_1^2D_{tot}(2\alpha D_{tot} - D_{tot} + S_{tot} - \alpha S_{tot})T_0^2 + (4\alpha K_1^2D_{tot}S_{tot} - \alpha K_1^2S_{tot}^2 - 4\alpha K_1^2D_{tot}^2 - 2K_1S_{tot} - 1)T_0 + 1 = 0 \quad (4)$$

$$\alpha K_1^2D_{tot}^2(1-\alpha)T_1^3 + 2K_1D_{tot}(1 - \alpha - \alpha K_1D_{tot})T_1^2 + (2\alpha K_1^2D_{tot}S_{tot} - \alpha K_1^2S_{tot}^2 - 2K_1D_{tot} - 2K_1S_{tot} - 1)T_1 + 2K_1S_{tot} = 0 \quad (5)$$

$$4\alpha K_1^2D_{tot}^2(1-\alpha)T_2^3 + 4K_1D_{tot}(\alpha^2K_1D_{tot} + \alpha^2K_1S_{tot} - \alpha K_1S_{tot} + 2\alpha - 2)T_2^2 + \alpha(4K_1^2D_{tot}S_{tot} - 4\alpha K_1^2D_{tot}S_{tot} - 4K_1^2D_{tot}^2 - \alpha K_1^2S_{tot}^2 - 2K_1S_{tot} - 4K_1D_{tot} - 1)T_2 + \alpha^2K_1^2S_{tot}^2 = 0 \quad (6)$$

Equations 4−6 have a role in this analysis analogous to that of the single quadratic equation that describes the fraction bound for simple single-site binding. In the single-site case, the real root of the quadratic equation gives the so-called "tight-binding equation" for the fraction bound, used in the nonlinear least-squares fitting algorithm to obtain the best fit parameters.[36]

In this cooperative binding case, the algebraic solutions of eqs 4−6 are complicated, and it is not clear in advance which, or indeed how many, of the three roots of each equation will have a real value, because this changes with the values of the equilibrium constants. Consequently, it is simpler to solve numerically for all three roots of each equation. This produces (usually) three possible values each of T_0, T_1, and T_2. However, only one combination of these values satisfies the following three physically necessary conditions: (i) T_0, T_1, and T_2 are each real, (ii) each has a value between 0 and 1, and (iii) $T_0 + T_1 + T_2 = 1$. This unique combination of values can be obtained for any given values of the parameters (S_{tot}, D_{tot}, K_1, and α). Consequently, numerical estimates of the partial derivatives of the fractional occupancies (i.e., changes arising from a small change in the parameters) can be made, and these are used in an otherwise standard nonlinear least-squares Levenberg−Marquardt algorithm[38] to obtain the best fit parameters. Error estimates for the parameter values are determined from the covariance matrix in the standard manner using the residuals as the error estimates in the data points.[38] Mathematica (Wolfram Inc.) scripts used in the analysis are available at http://people.cryst.bbk.ac.uk/~ubcg66a/software.html.

RESULTS AND DISCUSSION

Stoichiometry of the Simocyclinone D8−Gyrase A59 Complex. The nanoESI MS spectrum of GyrA59 alone was recorded under conditions suitable for the preservation of noncovalent interactions (Figure 2a). A well-resolved charge state series was observed, containing a single ion series centered at m/z 5580. Incubating GyrA59 with a 1.6-fold excess of SD8 (70 μM) gives a spectrum very similar to that obtained for the apoprotein; however, the charge states are shifted to higher m/z values (centered at m/z 5952), indicative of an increase in mass (Figure 2b). The average number of charges in the ion series has been reduced by one because of the addition of 0.5% (v/v) DMSO used to solubilize SD8. DMSO reduces the surface tension of the solution, and consequently, the droplet size from the ESI process is reduced, resulting in fewer charges on the gas-phase ion. Consequently, DMSO concentrations were minimized to ensure no disruption of protein structure took place as determined from the charge state profile (up to 1.6% DMSO we observed only small changes to the average charge and no change to the charge state distribution or appearance of the peaks.) The measured masses of 117214 ± 9 and 119060 ± 29 Da for the apo and ligand-bound species, respectively, compare well with those calculated from the sequence for the GyrA59 dimer (117217 Da) and the GyrA59 dimer bound to two SD8 molecules (119083 Da).

The spectra (Figure 2a) clearly show that the GyrA59 dimer is almost exclusively in the doubly bound state at an approximately

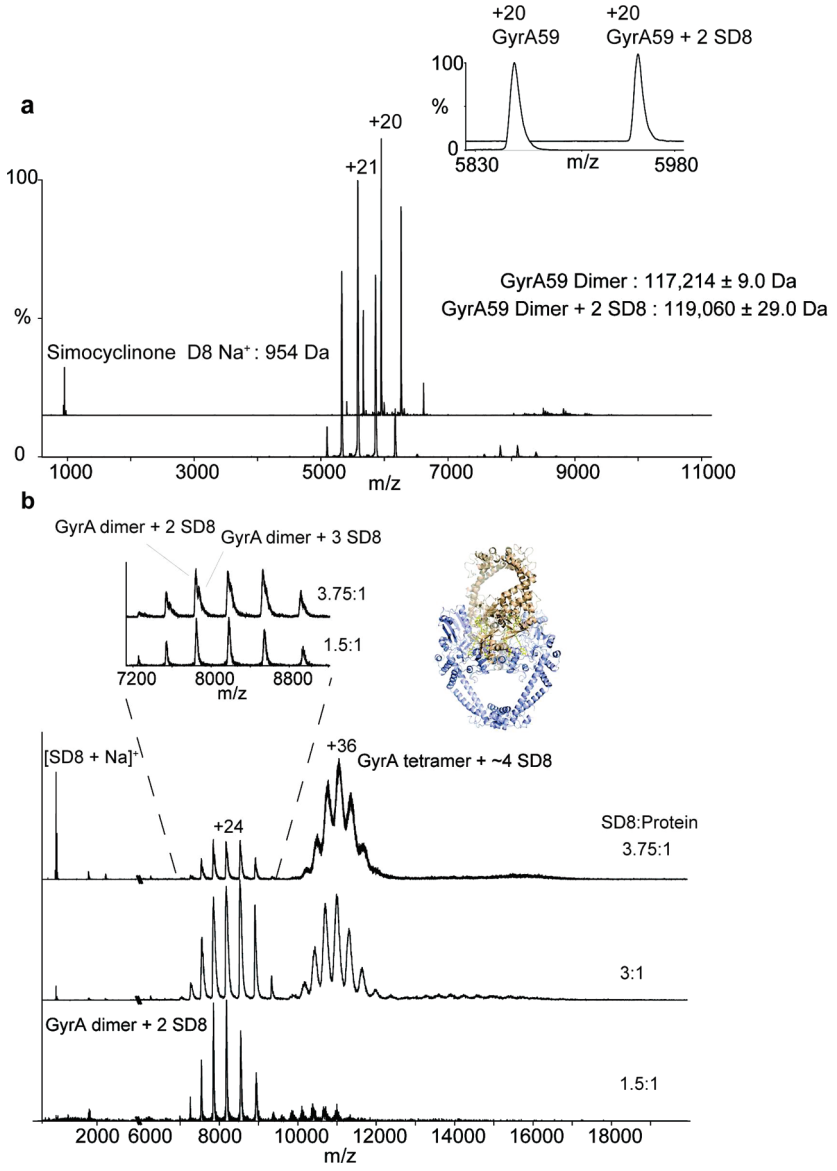

Figure 2. Nanoelectrospray ionization mass spectra of GyrA59 (a) alone (bottom trace) and after incubation with an excess of SD8 (top trace). A single ion series is observed, centered at m/z 5580. Incubation with SD8 shifts the charge state series to higher m/z values indicative of an increase in mass. The measured masses are consistent with the apo GyrA59 dimer and a bound species with a 1:1 ligand:subunit stoichiometry, which sees the GyrA59 dimer bound to two SD8 molecules. The singly charged ion at m/z 954 corresponds to unbound sodiated SD8. (b) Nanoelectrospray ionization mass spectra of the larger, full-length GyrA after addition of 1.5, 3, and 3.75 equiv of SD8. There is a progressive conversion of the GyrA dimer to a tetrameric species producing an ion series centered at m/z ~11000. The atomic model of the cross-linked tetramer was produced from the X-ray structure.[26]

1:1 SD8 ligand:subunit ratio indicative of a high-affinity interaction. We have previously shown, by analytical untracetrifugation and MS, that incubation of GyrA with higher molar equivalents of SD8 leads to the formation of a tetrameric species with four SD8 molecules bound (Figure 2b) and reported the crystal structure of this tetrameric form of the GyrA59−SD8 complex.[26]

Elucidating the Mechanism of Binding of SD8 to GyrA59. To gain further insight into the specific binding mechanism of SD8, we performed MS experiments using monofunctional fragments of the SD8 inhibitor molecule in complex with GyrA59.

Spectra obtained for 0.5 and 2 molar equiv of the polyketide containing simocyclinone C4 (SC4) and the aminocoumarin MGD8N2A (N2A) are shown in Figure 3.

It is clear that the interaction of SC4 with GyrA59 is substantially weaker than that of SD8. For 0.5 equiv of SC4, <50% of the GyrA59 dimers have any ligand bound and approximately 18% have both sites occupied. Only with 2 equiv of SC4 did a majority of the GyrA59 dimers form liganded complexes, although still short of saturation. There is no measurable population of the aminocoumarin-containing fragment MGD8N2A bound to GyrA59 at 0.5 equiv (we estimate from the peak widths that we would not be able to detect binding if this was at levels of <3−5%) and ~50% singly bound at 2 equiv. (There appears to be a small population of doubly bound ions on the +18 charge state at 2 equiv, but this is not apparent on the other charge states in the series.) The data obtained for the polyketide and aminocoumarin fragments of SD8 clearly

dx.doi.org/10.1021/bi101691k |*Biochemistry* 2011, 50, 3432–3440

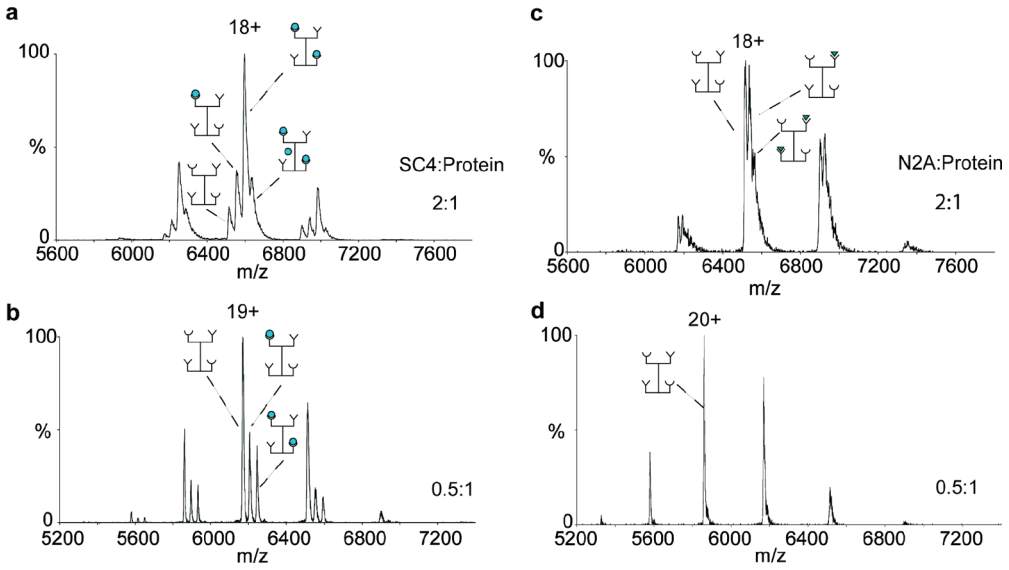

Figure 3. MS spectra obtained after titrations of GyrA59 with the monofunctional SD8 fragments SC4 (a and b) and N2A (c and d). The interaction of the PK-containing SC4 is substantially weaker than that of SD8. (b) At 0.5 equiv of inhibitor, SC4 has bound 44% of the GyrA59 dimers, with ~18% having both sites occupied. (a) With 2 equiv of SC4, ~72% of the GyrA59 dimers are doubly bound. (Of those, ~18% have bound a third molecule of SC4. This is believed to be a nonspecific interaction, possibly due to self-interaction with the bound lipophilic ligands.) The interaction of N2A with GyrA59 is the weakest of those of the three molecules studied. (d) There is no measurable population of N2A bound to GyrA59 at 0.5 equiv of inhibitor. (c) At 2 equiv of N2A, ~50% of the GyrA59 dimers have bound a single N2A ligand; however, there is a small population of ions with two N2A ligands bound on the +18 charge state, but we are unable to measure any such populations on the other charge states in the series (we estimate from the peak widths that we would not be able to detect binding if this was at levels of <3−5%).

demonstrate that the high-affinity binding of SD8 to GyrA59 is a function of both functional groups of SD8 and both binding pockets on each monomer of GyrA59.

These observations raise the question of whether the functional ends must be conjoined in one bifunctional molecule or if occupancy at both binding pockets is sufficient to promote an enhanced interaction. To directly address this, we titrated both SC4 and N2A fragments of SD8 into solutions of GyrA59. Given that each GyrA59 dimer has four binding sites, two for SC4 and two for N2A, there are 10 possible species that could be formed from a solution containing both fragments (Figure 4a). Of those, three possible populations will not be resolved as they are either isobaric at the experimental resolution or positional isomers. Isobaric ions were as follows: $(N2A)_2$ with SC4 (834.12 Da vs 722.22 Da) and $(SC4)(N2A)_2$ with $(SC4)_2$ (1556.34 Da vs 1444.44 Da). On the +18 charge state, these would produce pairs of peaks that differ by m/z 6.2, and the experimental peak width is m/z 18. A positional isomer of the SC4−N2A complex is also produced in which both fragments are located on one monomer or one on each. [The structure with three SC4 fragments bound is also isobaric with $(SC4)_2(N2A)_2$.]

The MS spectrum obtained after the addition of 2 equiv of both SC4 and N2A is shown in Figure 4b. As expected, the spectrum recorded for the titration with mixed fragments has charge states that are split into heptets (Figure 4b, inset). It is clear from a comparison of the spectra that there is no enhancement of binding when both fragments are added to GyrA59. It is difficult to analyze such (potentially) complex binding in a rigorous manner, but a simplistic analysis, assuming that SC4 binds with much higher affinity than N2A, gives an approximately 1:1:2 ratio of species without SC4 bound, singly bound to SC4, and doubly bound to SC4. In comparison with the previous data for SC4 alone (approximately 1:2:3), this ratio implies a somewhat reduced apparent affinity for SC4 in the presence of N2A. This may well arise because of interaction between the lipidic regions that both fragments contain.

Via comparison of the binding behavior of monofunctional fragments of SD8 added individually or in combination, we can unambiguously determine that high-affinity binding of SD8 to GyrA59 requires the covalent tethering of the two active ends of the molecule to form a bifunctional inhibitor.

Mass Spectrometry Reveals Positive Allosteric Cooperativity in SD8 Binding to GyrA. To further investigate the nature of the GyrA59−SD8 interaction, we performed a series of titrations involving the addition of SD8 to GyrA59 (Figure 5). Each charge state appears in the spectrum as a well-resolved triplet corresponding to the apo GyrA59 dimer, a singly bound SD8−GyrA59 dimer complex, and a doubly bound SD8−GyrA59 dimer complex. For the +19 charge state, the concentration of the singly bound GyrA59 dimer reaches a maximum at an ~0.5:1 ratio of molar equivalents and then begins to decrease and the doubly bound species saturates at an ~1.1:1 ratio of molar equivalents. It is striking that the population of the singly bound dimer is lower than the population of the doubly bound dimer even at low ligand concentrations. This behavior is not expected for independent binding sites, because it is statistically more likely that a dimer will bind one molecule rather than two at low inhibitor concentrations. This is strongly indicative of the presence of two nonindependent binding sites that are exhibiting positive cooperativity, where binding of the first molecule enhances the affinity of a second binding reaction.

Analysis of Cooperative Behavior Using MS Data. The unique ability of the MS titration experiments to allow the determination of the relative concentrations of each macromolecular species in solution allows the fractional populations of the apo and singly and doubly bound SD8−GyrA59 dimer complexes

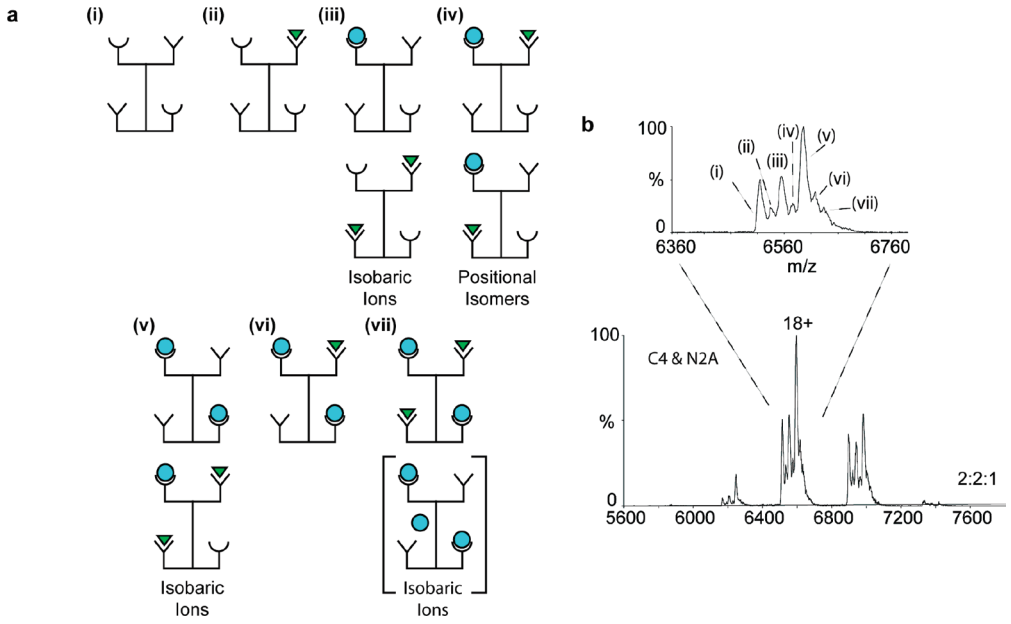

Figure 4. (a) Possible species formed from titration of GyrA59 with inhibitor fragments SC4 and N2A. There are 10 possible combinations of ligand-bound GyrA59 that may be formed after titration with both SC4 and N2A. Of those, three will not be resolved as they are either isobaric at the experimental resolution or positional isomers. An 11th structure represents a nonspecific complex in which three SC4 fragments are bound (in brackets). (b) MS spectra after titration of GyrA59 with both N2A and SC4 monofunctional fragments. The charge states are split into heptets (inset) and are labeled according to the scheme in panel a. There is little difference between the affinities of the fragments when added alone and when added in combination. From these data, we can unambiguously determine that the tight binding of SD8 to GyrA59 is a property of the tethering together of both active moieties of SD8 to form a hybrid bifunctional inhibitor.

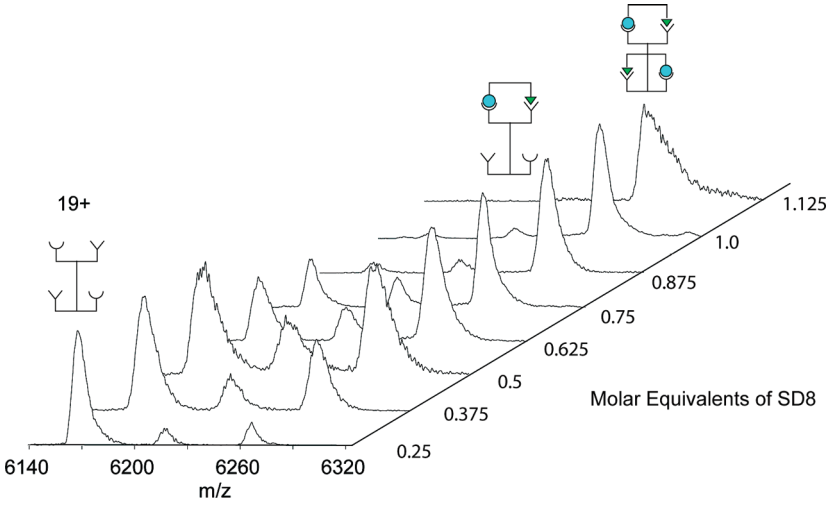

Figure 5. Mass spectra of GyrA59 after titration with its inhibitor SD8. Stack plot of the mass spectra of the +19 charge state of the GyrA59 dimer obtained for the full titration from 0.25 to 1.125 molar equiv of SD8 into a 44 μM solution of GyrA59. The charge states of the GyrA59 dimer appear as a well-resolved triplet corresponding to the apo GyrA59 dimer, a singly bound SD8−GyrA59 complex, and a doubly bound SD8−GyrA59 complex. From the spectra recorded at low SD8 concentrations, it is clear that there is a strong preference for formation of the doubly bound form of the dimer. This nonstatistical behavior is indicative of dependent binding sites exhibiting a strong positive cooperativity of binding.

to be plotted as a function of total ligand concentration (Figure 6). We measured the peak heights of all the charge states in the mass spectrum. Assuming equal ionization efficiencies for the apo and ligand-bound forms of the protein, we then estimated the fractions of each corresponding species in solution, the apo state (T_0), the singly bound state (T_1), and the doubly bound species (T_2). As we know the total concentration of dimeric protein (D_{tot}) and ligand (S_{tot}) at each step in the titration, we are able to simultaneously fit the data to a theoretical model in terms of their common parameters, i.e., the total concentrations, binding constants for the first and second binding events, and the degree of cooperativity of the interaction.

A simple phenomenological model for cooperativity in a constitutive dimer[27] is provided by the scheme in Figure 6a. It is worth noting that this simple scheme is compatible with both the classic MWC[39] and KNF[40] models for cooperativity, making

dx.doi.org/10.1021/bi101691k |*Biochemistry* 2011, 50, 3432–3440

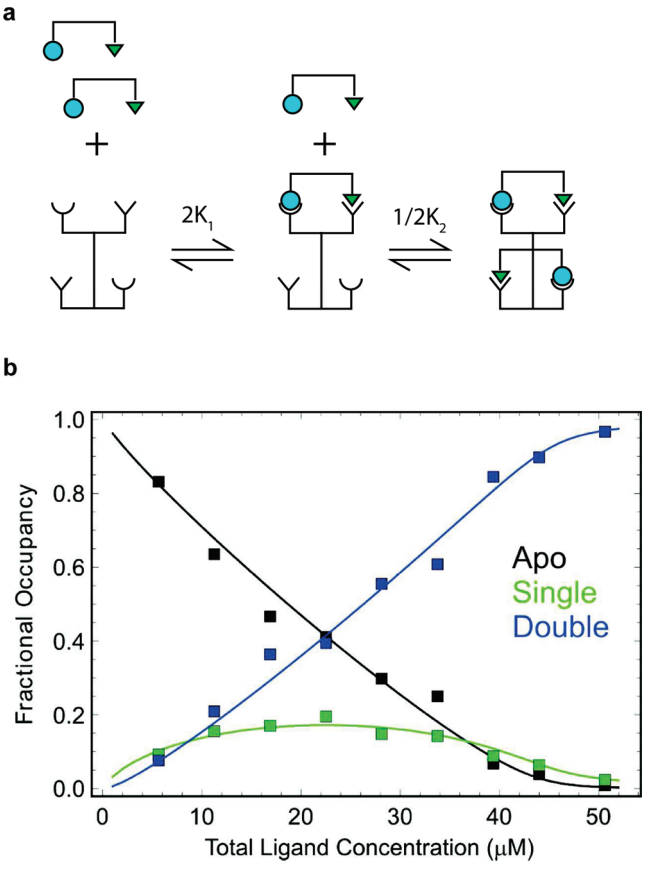

Figure 6. Analysis of cooperative binding of SD8. Reaction scheme (a). Fraction of dimers in the apo, singly bound, and doubly bound states. (b) Fitted curves are overlaid on experimental data points for a subunit concentration of 44 μM. The best fit association constant for the first binding event (K_1) is $(4.47 \pm 0.26) \times 10^5$ M^{-1} and for the second ligand binding (K_2) $(1.03 \pm 0.10) \times 10^7$ M^{-1}.

no assumption about the physical mechanism other than that prior to binding the two subunits are equivalent. Here

$$K_1 = T_1/(2T_0S) \quad (7)$$

$$K_2 = (2T_2)/(T_1S) \quad (8)$$

where S is the free ligand concentration, K_1 the association constant for the first ligand to bind, and K_2 the association constant for the second ligand.[27] The factors of 2 in these definitions of the equilibrium constants arise because there are two ways of binding a ligand to the apo state dimer to create a singly bound state and two ways of dissociating a doubly bound state to create a singly bound state.[39] The degree of cooperativity is defined as

$$\alpha = K_2/K_1 \quad (9)$$

If binding to each site is independent, $\alpha = 1$; if the binding is positively cooperative, $\alpha > 1$, and if the binding is negatively cooperative, $\alpha < 1$. The free ligand concentration is not measured in MS experiments but is related to the known total concentrations of the dimeric protein (D_{tot}) and ligand (S_{tot}) and measured fractional populations of the bound states at each step in the titration

$$S = S_{tot} - D_{tot}T_1 - 2D_{tot}T_2 \quad (10)$$

The excellent quality of the data and a newly developed tight-binding analysis and fitting method (see Experimental Procedures for details) allow us to simultaneously fit the fractional populations of each species to the theoretical model in terms of K_1, K_2, S_{tot}, and D_{tot} (Figure 6b). The binding is found to be highly positively cooperative with an α of 23 ± 0.7, with a low micromolar dissociation constant for the first binding event ($K_d = 2.2$ μM) and a submicromolar dissociation constant for the second ligand ($K_d = 97$ nM); this is consistent with the affinity previously determined by surface plasmon resonance.[26] Consequently, the highly effective inhibition of gyrase by SD8 ($IC_{50} = 0.6$ μM)[26] is dependent on positive cooperativity in its binding.

Although fewer data and a smaller portion of their binding curves are available from the MS data on the SC4 and N2A fragments, the cooperative binding analysis described above can also be applied in those cases. The results of this give a K_d of 42.3 μM and an α of 6.5 for the PK-containing SC4 fragment (errors from the fit are ~10%). For the N2A fragment, we estimate a K_d of 210 μM (given that this is effectively determined from a single data point the error is at least 15%) and find no evidence of any significant cooperativity (although given the difficulties in accurately quantitating the doubly bound species some small effect cannot be ruled out). We can say that the cooperativity seems to arise mostly from binding of the polyketide group.

SD8 Binds to Gyrase in a Bent-Over Conformation. The data we have obtained have allowed us to validate our previous proposed model for the binding of SD8 to GyrA59, which explains the high inhibitory activity and takes into account our observations of positive cooperativity and the unusual tetramerization of the complex at high inhibitor concentrations. The relative affinities of the constituent fragments of SD8 suggest that the most likely binding scenario is one in which the initial binding of the higher-affinity polyketide group anchors SD8 to GyrA59, introducing a beneficial localization effect (sometimes also called a configurational cooperativity), i.e., the local concentration of the low-affinity aminocoumarin is enhanced by this polyketide anchor (Figure 7).

The only sterically possible arrangement of SD8 that can account for the requirement of both binding ends interacting with GyrA59 is one in which both sites on a single monomer are occupied by a single molecule of SD8. We have modeled this starting from our recent crystal structure; treating the protein as a rigid entity, we are able to place two ligands in a bent-over conformation to maintain the crystallographically observed interactions at each of the PK and AC binding sites[26] without invoking any substantial conformational change to the protein.

MS data have shown that the binding of the polyketide fragment is weakly allosterically cooperative with binding at the second polyketide site, being enhanced by binding at the first. In the context of the bifunctional SD8, this cooperativity is strengthened. The bent-over conformation introduces "strain" into the SD8 linker that could cause small structural changes in the protein sufficient to account for the additional cooperative interplay between the binding sites on adjacent monomers.

We have reported a detailed mass spectrometric evaluation of the mechanism by which SD8 binds to the A subunit of DNA gyrase, the results of which have allowed us to validate an alternative mechanism of binding to the one observed by X-ray crystallography. MS studies have shown that at pharmaceutically relevant concentrations the dimeric protein binds SD8 with a stoichiometry of 1:1, and experiments with fragments of SD8 have revealed that the polyketide moiety interacts with GyrA59 with a 5-fold greater affinity than the aminocoumarin moiety.

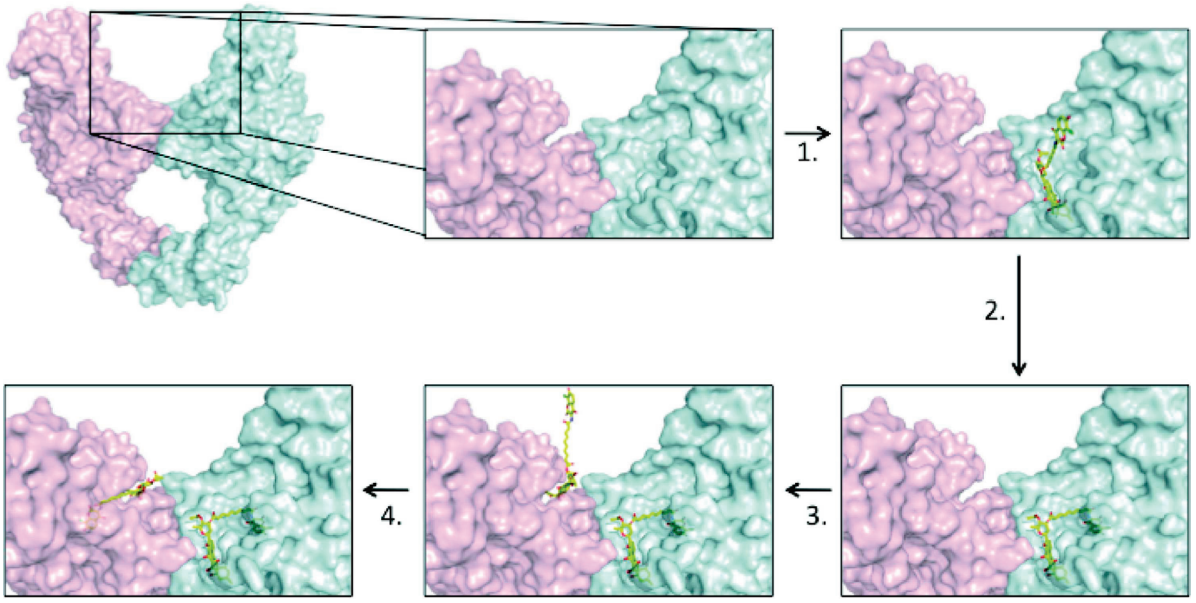

Figure 7. Bent-over binding model. (1) The initial binding of the higher-affinity polyketide anchors SD8 to GyrA59. (2) The local concentration of the low-affinity aminocoumarin is enhanced by this anchor, leading to occupation of both binding pockets in a single monomer. (3 and 4) It is proposed that both a response to the polyketide binding in one pocket and strain in the arched over SD8 induce conformational changes in the protein that can modify the binding pocket on the second GyrA59 subunit, making it easier for a second SD8 molecule to bind in a manner akin to that of the first.

Furthermore, these interactions are significantly weaker than that of the bifunctional SD8. There is no enhancement of the affinity of each functional moiety in samples containing both inhibitor fragments, demonstrating that the high-affinity binding requires conjoining both functional ends in a single molecule. The enhanced affinity of the bifunctional molecule can be thought to result in part from an increase in the local concentration of the AC moiety through anchoring by the PK moiety. Further, we are able to quantitatively analyze the MS data to show that allosteric cooperativity produces a >20-fold enhancement in the affinity of the bifunctional antibiotic binding to the second subunit following the binding of the first. This produced estimates of the dissociation constants for both binding events (K_d = 2.2 μM for the first and K_d = 97 nM for the second). Together, the allosteric cooperativity between binding sites on adjacent gyrase subunits and local concentration effects inherent in a bifunctional molecule binding at two neighboring sites provide a mechanistic explanation of the high affinity of SD8. The mass spectrometry methodology we have established here provides a rigorous and general approach to the direct estimation of the dissociation constants and a quantitative estimation of cooperative effects in dimeric systems and provides the basis for extension to helping unravel the complexities of systems with larger numbers of binding sites.

AUTHOR INFORMATION

Corresponding Author

*E-mail: adam.mckay@ucl.ac.uk. Phone: 0207 679 4667. Fax: 0207 679 7463.

Present Addresses

[||]School of Biological Sciences, University of East Anglia, Norwich NR4 7TJ, U.K.

Author Contributions

This study was conceived by A.M. and A.R.M. Experimental work was conducted by M.J.E. and A.R.M. Analytical tools were developed by M.A.W. Data analysis was performed by M.A.W. and A.R.M. A.M., M.A.W., and A.R.M. wrote the manuscript.

Funding Sources

M.J.E. was supported by a BBSRC-CASE studentship funded by BBSRC (U.K.) and Plant Bioscience Limited. A.R.M. is supported by a Research Councils UK fellowship and the Wellcome Trust (090225/Z/09/Z). A.M. is supported by BBSRC.

ACKNOWLEDGMENT

We thank Stephen Bornemann, Steve Caddick, Stefan Howorka, David Lawson, and Andrew Maxwell for helpful discussions and for comments on the manuscript. We thank Hans-Peter Fiedler and Axel Zeeck for gifts of compounds.

ABBREVIATIONS

AC, aminocoumarin; DMSO, dimethyl sulfoxide; D_{tot}, concentration of the dimeric protein; GyrA, A subunit of *E. coli* DNA gyrase; GyrA59, 59 kDa N-terminal domain of GyrA; GyrB, B subunit of *E. coli* DNA gyrase; IC_{50}, half-maximal inhibitory concentration; K_d, dissociation constant; MS, mass spectrometry; N2A, MGD8N2A (simocyclinone D8 lacking the polyketide moiety); PK, polyketide; SC4, simocyclinone C4 (simocyclinone D8 lacking the aminocoumarin moiety); SD8, simocyclinone D8; S_{tot}, total ligand concentration.

REFERENCES

(1) Ruotolo, B. T., Giles, K., Campuzano, I., Sandercock, A. M., Bateman, R. H., and Robinson, C. V. (2005) Evidence for macromolecular protein rings in the absence of bulk water. *Science 310*, 1658–1661.

(2) Leary, J. A., Schenauer, M. R., Stefanescu, R., Andaya, A., Ruotolo, B. T., Robinson, C. V., Thalassinos, K., Scrivens, J. H., Sokabe, M., and Hershey, J. W. (2009) Methodology for measuring conformation of solvent-disrupted protein subunits using T-WAVE ion mobility

MS: An investigation into eukaryotic initiation factors. *J. Am. Soc. Mass Spectrom. 20*, 1699–1706.

(3) Scarff, C. A., Patel, V. J., Thalassinos, K., and Scrivens, J. H. (2009) Probing hemoglobin structure by means of traveling-wave ion mobility mass spectrometry. *J. Am. Soc. Mass Spectrom. 20*, 625–631.

(4) Scarff, C. A., Thalassinos, K., Hilton, G. R., and Scrivens, J. H. (2008) Travelling wave ion mobility mass spectrometry studies of protein structure: Biological significance and comparison with X-ray crystallography and nuclear magnetic resonance spectroscopy measurements. *Rapid Commun. Mass Spectrom. 22*, 3297–3304.

(5) Smith, D. P., Knapman, T. W., Campuzano, I., Malham, R. W., Berryman, J. T., Radford, S. E., and Ashcroft, A. E. (2009) Deciphering drift time measurements from travelling wave ion mobility spectrometry-mass spectrometry studies. *Eur. J. Mass Spectrom. 15*, 113–130.

(6) Ruotolo, B. T., and Robinson, C. V. (2006) Aspects of native proteins are retained in vacuum. *Curr. Opin. Chem. Biol. 10*, 402–408.

(7) Heck, A. J. (2008) Native mass spectrometry: A bridge between interactomics and structural biology. *Nat. Methods 5*, 927–933.

(8) Heck, A. J., and Van Den Heuvel, R. H. (2004) Investigation of intact protein complexes by mass spectrometry. *Mass Spectrom. Rev. 23*, 368–389.

(9) Hernandez, H., and Robinson, C. V. (2007) Determining the stoichiometry and interactions of macromolecular assemblies from mass spectrometry. *Nat. Protoc. 2*, 715–726.

(10) Loo, J. A. (1997) Studying noncovalent protein complexes by electrospray ionization mass spectrometry. *Mass Spectrom. Rev. 16*, 1–23.

(11) Sharon, M., and Robinson, C. V. (2007) The role of mass spectrometry in structure elucidation of dynamic protein complexes. *Annu. Rev. Biochem. 76*, 167–193.

(12) McCammon, M. G., and Robinson, C. V. (2004) Structural change in response to ligand binding. *Curr. Opin. Chem. Biol. 8*, 60–65.

(13) Bligh, S. W., Haley, T., and Lowe, P. N. (2003) Measurement of dissociation constants of inhibitors binding to Src SH2 domain protein by non-covalent electrospray ionization mass spectrometry. *J. Mol. Recognit. 16*, 139–148.

(14) Tjernberg, A., Carno, S., Oliv, F., Benkestock, K., Edlund, P. O., Griffiths, W. J., and Hallen, D. (2004) Determination of dissociation constants for protein-ligand complexes by electrospray ionization mass spectrometry. *Anal. Chem. 76*, 4325–4331.

(15) Daniel, J. M., Friess, S. D., Rajagopalan, S., Wendt, S., and Zenobi, R. (2002) Quantitative determination of noncolvant binding interactions using soft ionisation mass spectrometry. *Int. J. Mass Spectrom. 216*, 1–27.

(16) Bates, A., and Maxwell, A. (2005) *DNA Topology*, 2nd ed., Oxford University Press, New York.

(17) Schoeffler, A. J., and Berger, J. M. (2008) DNA topoisomerases: Harnessing and constraining energy to govern chromosome topology. *Q. Rev. Biophys. 41*, 41–101.

(18) Nollmann, M., Crisona, N. J., and Arimondo, P. B. (2007) Thirty years of *Escherichia coli* DNA gyrase: From in vivo function to single-molecule mechanism. *Biochimie 89*, 490–499.

(19) Pommier, Y. (2009) DNA topoisomerase I inhibitors: Chemistry, biology, and interfacial inhibition. *Chem. Rev. 109*, 2894–2902.

(20) Gatto, B., Capranico, G., and Palumbo, M. (1999) Drugs acting on DNA topoisomerases: Recent advances and future perspectives. *Curr. Pharm. Des. 5*, 195–215.

(21) Maxwell, A. (1999) DNA gyrase as a drug target. *Biochem. Soc. Trans. 27*, 48–53.

(22) Flatman, R. H., Howells, A. J., Heide, L., Fiedler, H. P., and Maxwell, A. (2005) Simocyclinone D8, an inhibitor of DNA gyrase with a novel mode of action. *Antimicrob. Agents Chemother. 49*, 1093–1100.

(23) Holzenkampfer, M., Walker, M., Zeeck, A., Schimana, J., and Fiedler, H. P. (2002) Simocyclinones, novel cytostatic angucyclinone antibiotics produced by *Streptomyces antibioticus* Tu 6040 II. Structure elucidation and biosynthesis. *J. Antibiot. 55*, 301–307.

(24) Schimana, J., Fiedler, H. P., Groth, I., Sussmuth, R., Beil, W., Walker, M., and Zeeck, A. (2000) Simocyclinones, novel cytostatic angucyclinone antibiotics produced by *Streptomyces antibioticus* Tu 6040. I. Taxonomy, fermentation, isolation and biological activities. *J. Antibiot. 53*, 779–787.

(25) Theobald, U., Schimana, J., and Fiedler, H. P. (2000) Microbial growth and production kinetics of *Streptomyces antibioticus* Tu 6040. *Antonie van Leeuwenhoek 78*, 307–313.

(26) Edwards, M. J., Flatman, R. H., Mitchenall, L. A., Stevenson, C. E., Le, T. B., Clarke, T. A., McKay, A. R., Fiedler, H. P., Buttner, M. J., Lawson, D. M., and Maxwell, A. (2009) A crystal structure of the bifunctional antibiotic simocyclinone D8, bound to DNA gyrase. *Science 326*, 1415–1418.

(27) Hunter, C. A., and Anderson, H. L. (2009) What is cooperativity? *Angew. Chem., Int. Ed. 48*, 7488–7499.

(28) Whitty, A. (2008) Cooperativity and biological complexity. *Nat. Chem. Biol. 4*, 435–439.

(29) Potier, N., Rogniaux, H., Chevreux, G., and Van Dorsselaer, A. (2005) Ligand−metal ion binding to proteins: Investigation by ESI mass spectrometry. *Methods Enzymol. 402*, 361–389.

(30) McCammon, M. G., Scott, D. J., Keetch, C. A., Greene, L. H., Purkey, H. E., Petrassi, H. M., Kelly, J., and Robinson, C. V. (2002) Screening transthyretin amyloid fibril inhibitiors: Characterization of novel multiprotein multiligand complexes by mass spectrometry. *Structure 10*, 851–863.

(31) Rogniaux, H., Sanglier, S., Strupat, K., Azza, S., Roitel, O., Ball, V., Tritsch, D., Branlant, G., and Van Dorsselaer, A. (2001) Mass spectrometry as a novel approach to probe cooperativity in multimeric enzymatic systems. *Anal. Biochem. 291*, 48–61.

(32) Maxwell, A., and Howells, A. J. (1999) Overexpression and purification of bacterial DNA gyrase. *Methods Mol. Biol. 94*, 135–144.

(33) Reece, R. J., and Maxwell, A. (1991) Probing the limits of the DNA breakage-reunion domain of the *Escherichia coli* DNA gyrase A protein. *J. Biol. Chem. 266*, 3540–3546.

(34) Edwards, M. J., Flatman, R. H., Mitchenall, L. A., Stevenson, C. E., Maxwell, A., and Lawson, D. M. (2009) Crystallization and preliminary X-ray analysis of a complex formed between the antibiotic simocyclinone D8 and the DNA breakage-reunion domain of *Escherichia coli* DNA gyrase. *Acta Crystallogr. F65*, 846–848.

(35) Williams, J. W., and Morrison, J. F. (1979) The kinetics of reversible tight-binding inhibition. *Methods Enzymol. 63*, 437–467.

(36) Copeland, R. A. (2005) Tight binding inhibition. In *Evaluation of enzyme inhibitors in drug discovery*, pp 178−213, John Wiley and Sons Inc., New York.

(37) Swillens, S. (1995) Interpretation of binding curves obtained with high receptor concentrations: Practical aid for computer analysis. *Mol. Pharmacol. 47*, 1197–1203.

(38) Press, W. H., Teukolsky, S. A., Vetterling, W. T., and Flannery, B. P. (2007) *Numerical Recipies: The Art of Scientific Computing*, 3rd ed., Cambridge University Press, Cambridge, U.K.

(39) Monod, J., Wyman, J., and Changeux, J. P. (1965) On the Nature of Allosteric Transitions: A Plausible Model. *J. Mol. Biol. 12*, 88–118.

(40) Koshland, D. E., Jr., Nemethy, G., and Filmer, D. (1966) *Biochemistry 5*, 365–85.